



## Dynamics of riverine CO<sub>2</sub> in the Yangtze River fluvial network and their implications for carbon evasion

Lishan Ran<sup>1,2</sup>, Xi Xi Lu<sup>2,3,\*</sup>, Shaoda Liu<sup>2</sup>

5 <sup>1</sup>Department of geography, the University of Hong Kong, Pokfulam Road, Hong Kong

<sup>2</sup>Department of geography, National University of Singapore, 117570, Singapore

<sup>3</sup>College of Environment & Resources, Inner Mongolia University, Hohhot, 010021, China

\*Correspondence: [geoluxx@nus.edu.sg](mailto:geoluxx@nus.edu.sg)

10 **Abstract:** Understanding riverine carbon dynamics is critical for not only better estimates of various carbon fluxes but also evaluating their significance in the global carbon budget. As an important pathway of global land-ocean carbon exchange, the Yangtze River has received less attention regarding its vertical carbon evasion than lateral transport. Using long-term water chemistry data, we calculated CO<sub>2</sub> partial pressure (*p*CO<sub>2</sub>) from pH and alkalinity and examined

15 its spatial and temporal dynamics and the impacts of environmental settings. With alkalinity ranging from 415 to >3400 μmol L<sup>-1</sup>, the river waters were supersaturated with dissolved CO<sub>2</sub>, generally 2–20 folds the atmospheric equilibrium (i.e., 390 μatm). Changes of *p*CO<sub>2</sub> were collectively controlled by terrestrial ecosystems, hydrological regime, and rock weathering. High *p*CO<sub>2</sub> values were observed spatially in catchments with abundant carbonate presence and

20 seasonally in the wet season when recent-fixed organic matter was exported into the river network. In-stream processing of organic matter facilitated CO<sub>2</sub> production and sustained the high *p*CO<sub>2</sub>, although the alkalinity presented an apparent dilution effect with lower alkalinity concentrations in higher flow periods. The decreasing *p*CO<sub>2</sub> from the smallest headwater streams through tributaries to the mainstream illustrates the significance of direct terrestrial carbon input

25 in controlling riverine carbon. With a basin-wide mean *p*CO<sub>2</sub> of 2662±1240 μatm, substantial



CO<sub>2</sub> evasion from the Yangtze River fluvial network is expected. Future research efforts are thus needed to quantify the amount of CO<sub>2</sub> evasion and assess its biogeochemical implications for watershed-scale carbon cycle. In view of the Yangtze River's relative importance in global carbon export, its CO<sub>2</sub> evasion would be significant for global carbon budget.

30 **Keywords:** CO<sub>2</sub> partial pressure ( $p\text{CO}_2$ ); riverine carbon cycle; spatial and temporal patterns; CO<sub>2</sub> evasion; Yangtze River

## 1. Introduction

Inland waters, including rivers, streams, lakes, wetland, and reservoirs, have recently been  
35 recognized as active components of the global carbon cycle, transporting, storing, and processing huge amounts of terrestrially-derived carbon (Aufdenkampe et al., 2011; Cole et al., 2007; Raymond et al., 2013; Richey et al., 2002; Weyhenmeyer et al., 2015; Borges et al., 2015). With a higher CO<sub>2</sub> partial pressure ( $p\text{CO}_2$ ) than the atmospheric equilibrium (i.e., 390  $\mu\text{atm}$ ), inland waters are mostly net carbon sources to the atmosphere. Published studies show that the  
40 annually degassed CO<sub>2</sub> from inland waters is estimated to almost entirely compensate the total annual carbon uptake by ocean systems (Wanninkhof et al., 2013; Regnier et al., 2013). Global estimates of CO<sub>2</sub> evasion from rivers and streams range from 0.56 to 1.8 PgC yr<sup>-1</sup> (Aufdenkampe et al., 2011; Raymond et al., 2013; Lauerwald et al., 2015). It is apparent that these results vary considerably and are associated with great uncertainties. The most recent estimate of 0.65 PgC  
45 yr<sup>-1</sup> by Lauerwald et al. (2015) accounts for only 36% of the efflux estimate made by Raymond et al. (2013), although they used the same water chemistry data set. Among the numerous factors



contributing to current CO<sub>2</sub> evasion uncertainties, a principal reason is the absence of a spatially explicit *p*CO<sub>2</sub> data set that covers the full spectrum of the global river and stream network.

50 Existing global maps of CO<sub>2</sub> evasion from fluvial network are typically generated on the basis of incomplete spatial coverage of *p*CO<sub>2</sub>, in which Asian rivers are heavily underrepresented (e.g., Aufdenkampe et al., 2011; Battin et al., 2009; Lauerwald et al., 2015; Raymond et al., 2013). Due to lack of direct *in situ* measurements, simplified extrapolation is normally used to predict *p*CO<sub>2</sub> in and CO<sub>2</sub> evasion from Asian river systems. Consequently, the estimation accuracy is

55 problematic and even erroneous. For example, for the Yellow River in East Asia, while the calculated *p*CO<sub>2</sub> from river water chemistry records is 2800 μatm (Ran et al., 2015a), the modeled *p*CO<sub>2</sub> by Lauerwald et al. (2015) is 30% lower (i.e., <2000 μatm). A much lower estimate of <700 μatm can be derived from the *p*CO<sub>2</sub> map produced in Raymond et al. (2013). Such great discrepancies are largely because riverine *p*CO<sub>2</sub> is highly site-specific and affected by

60 a wide range of environmental factors (e.g., Abril et al. 2015; Teodoru et al., 2015). Asian rivers are significant contributors to global carbon export, accounting for 40% of the global carbon flux from land to sea (Schlünz and Schneider, 2000; Hope et al., 1994). Estimating the amount of CO<sub>2</sub> degassed from Asian rivers is critical for global CO<sub>2</sub> evasion assessments. Recent work in

Mekong and Yellow rivers has demonstrated high *p*CO<sub>2</sub> and CO<sub>2</sub> effluxes (Alin et al., 2011; Ran

65 et al., 2015b), further highlighting the necessity of incorporating the currently underrepresented Asian rivers into global carbon budget assessments.



As an important carbon contributor to the West Pacific Ocean, the Yangtze River has received widespread attention in fluvial carbon export at various spatial and temporal scales. Studies of  
70 flux estimates of different carbon species date back to the early 1980s (Cauwet and Mackenzie, 1993; Gan et al., 1983; Milliman et al., 1984; Wang et al., 2012; Zhang et al., 2014; Ittekkot, 1988). Intensive observations covering seasonal variability show that the Yangtze River transports approximately 20 Mt of carbon per year into the oceans (Wu et al., 2007; Bao et al., 2015). Contrary to the long history of lateral export measurements, however, few studies have examined  
75 the vertical carbon exchange between the river system and the atmosphere (Li et al., 2012; Zhao et al., 2013; Chen et al., 2008). This is by nature largely due to the differences in sampling strategy. Unlike the lateral export that only involves measurements on the mainstream or at specific sites near the river mouth, quantifying basin-wide CO<sub>2</sub> evasion requires a spatially explicit *p*CO<sub>2</sub> data set encompassing the entire fluvial network. Any attempts of using limited  
80 local measurements to up-scale to the watershed scale are challenging and subject to large uncertainties. This has impacted the understanding of riverine carbon cycle within the Yangtze River watershed as well as its links to the atmosphere and ocean systems.

By using long-term water chemistry data measured in the Yangtze River basin, we calculated the  
85 riverine *p*CO<sub>2</sub> from pH and alkalinity. In combination with hydrologic and geologic information, the objectives of this study were to 1) investigate the spatial and temporal patterns of *p*CO<sub>2</sub> under ‘natural’ processes before significant human perturbations, mainly dam impoundment and land use changes since the 1990s; 2) to explore the couplings between *p*CO<sub>2</sub> and environmental



settings by investigating environmental and geomorphologic controls. Based on the obtained  
90  $p\text{CO}_2$ , we further evaluated its implications for  $\text{CO}_2$  evasion. In view of the Yangtze River's role  
in global fluvial export of water, sediment, and carbon (Syvitski et al., 2005; Wang et al., 2012),  
its  $\text{CO}_2$  evasion would be globally substantial. This  $p\text{CO}_2$  database is thus helpful to examine the  
spatial distribution of global riverine  $p\text{CO}_2$  and to refine global  $\text{CO}_2$  evasion from river systems.

## 95 2. Material and methods

### 2.1 The Yangtze River basin

With a length of 6380 km, the Yangtze River is the longest river in China and the third longest in  
the world. The river originates on the Tibetan Plateau and flows eastward through the Sichuan  
Basin and the Middle-Lower Reach Plains, before emptying into the East China Sea (Fig. 1a). Its  
100 drainage area is 1.81 million  $\text{km}^2$ . The Yangtze River basin is mainly overlain by sedimentary  
rocks that are composed of marine carbonates, evaporites, and continental deposits. Carbonates  
are widely distributed within the watershed and are particularly abundant in the Wujiang,  
Yuanjiang, and Hanjiang tributary catchments (Fig. 1b). Silicates are also widely present in the  
basin while metamorphic rocks are mainly scattered in the middle-lower reach (Fig. 1b). The  
105 Yangtze River is joined by a number of large tributaries, including the Yalongjiang, Daduhe,  
Minjiang, Jialingjiang, Wujiang, Yuanjiang, Xiangjiang, Hanjiang, and Ganjiang rivers (Fig. 1a).

#### Figure 1

Except the headwater region characterized by high elevation and cold climate (annual mean  
temperature  $<4\text{ }^\circ\text{C}$ ), the remaining watershed is affected by a subtropical monsoon climate with



110 the annual mean temperature in the middle-lower reach varying from 16 to 18 °C (Chen et al.,  
2002). Rainfall is the major source of water discharge, whereas snowfall supply is only  
significant in the ice-covered upstream mountainous areas. With a mean precipitation of 1100  
mm yr<sup>-1</sup>, the precipitation is spatially highly variable, decreasing from 1644 mm yr<sup>-1</sup> in the  
lower reach, to 1396 mm yr<sup>-1</sup> in the middle reach, and 435 mm yr<sup>-1</sup> in the upper reach (Chetelat  
115 et al., 2008). Approximately 60% of the annual precipitation falls during the wet season from  
June to September. Affected by summer monsoon, the wet season generally occurs earlier in the  
middle and lower reaches than in the inland upper reach. The water discharge from the upper to  
the lower reach presents a strong seasonal variability (Fig. 2). Monthly peak discharge occurs in  
July and can be 5–7 times greater than the lowest discharge in the dry season. The mean  
120 discharge at Datong station is 28,200 m<sup>3</sup> s<sup>-1</sup> (see its location in Fig. 3b), and consequently the  
Yangtze River annually discharges 889 km<sup>3</sup> of water into the ocean (Yang et al., 2002).

## Figure 2

### 2.2 Water chemistry data

Concentrations of alkalinity, major ions, and dissolved silica measured at 359 stations in the  
125 Yangtze River watershed (Fig. 1a) during the period 1960s–1985 were retrieved from the  
Hydrological Yearbooks, which were yearly produced by the Yangtze River Conservancy  
Commission (YRCC) for internal use. Other environmental variables concurrently measured at  
each sampling event, including pH, water temperature, and water discharge, were also extracted  
from the yearbooks for this study. The water samples for pH and temperature measurement were  
130 taken in the same period as these for ion analysis. The sampling frequency ranged from 1 to 14



times per month depending on flow conditions. Sampling at some stations during the period  
1966–1975 was less frequent. About 80% of the 359 stations have been continuously sampled  
for at least 10 years, starting from the early 1970s. To avoid severe river pollution by human  
activity, only the samples collected prior to 1985 were used. In addition, samples with the pH  
135 lower than 6.5 were manually discarded because the calculated  $p\text{CO}_2$  would be greatly biased  
due to contributions of noncarbonated alkalinity such as organic acid anions (Abril et al.,  
2015; Hunt et al., 2011). Because reservoir trapping and increased water residence time can  
remarkably alter the physical and biogeochemical properties of running water (Kemenes et al.,  
2011; Barros et al., 2011), the stations located inside or shortly below reservoirs were also  
140 intentionally removed. Given the tidal influences, mainstream stations downstream of Datong,  
626 km inland from the coast, were also excluded, as were the stations in the delta region that  
were affected either by tides or by intersections with other rivers via artificial canals. Based on  
these selection criteria, 339 stations, including 13 mainstream stations and 326 tributary stations,  
were retained and 47,809 water chemistry measurements in total were compiled.

145

Chemical analyses of water samples were performed under the authority of YRCC following the  
standard procedures and protocols described by Alekin et al. (1973) and the American Public  
Health Association (1985). While pH and temperature were measured in the field, the alkalinity  
was determined by acid titration. Detailed sampling and analysis procedures were presented in  
150 Chen et al. (2002). One important issue regarding historical records is data reliability. No  
assessment reports on quality assurance and quality control are available in the hydrological



yearbooks. An effective evaluation approach is to compare the hydro-chemical differences for samples collected at the same station but by different agencies. The Wuhan station on the Yangtze mainstream has also been monitored under the United Nations GEMS/Water Programme since 1980 (only yearly means available at <http://www.unep.org/gemswater>). The pH value from the yearbooks agreed well with that measured by the GEMS/Water Programme with <1.8% differences, while the alkalinity discrepancy between the two data sets is larger (Table 1). The yearbooks report a slightly higher alkalinity than the GEMS/Water Programme results by 7.6–13.9%, indicating that the yearbook reports are reliable for  $p\text{CO}_2$  calculation. High data quality of the yearbook reports can also be validated from comparison of major dissolved elements measured by the two agencies at Wuhan station (see Chen et al., 2002).

### Table 1

#### 2.3 Calculation of $p\text{CO}_2$

The conventional method of calculating  $p\text{CO}_2$  from pH and alkalinity was used. With ~90% of the measured pH ranging from 7.1 to 8.3 suggestive of natural process for the Yangtze River, bicarbonates were assumed equivalent to alkalinity (Amiotte-Suchet et al., 2003) because 96% of the alkalinity was dominated by bicarbonates. This approximation has been frequently used in Chinese river systems (Yao et al., 2007; Li et al., 2012; Ran et al., 2015a). The  $p\text{CO}_2$  was then calculated using CO2SYS program (Lewis and Wallace, 1998). However, using this method would produce biased extreme values that are unrealistic in natural river systems (Hunt et al., 2011; Weyhenmeyer et al., 2015). We thus reported median values per sampling station instead of means to avoid the impact of erroneous extreme results.





### 3. Results

#### 175 3.1 Spatio-temporal variability of alkalinity and $p\text{CO}_2$

Except the excluded measurements, pH in the Yangtze River waters varied from 6.5 to 9.2 with 96% of the pH measurements ranging from 7.3 to 8.3 (Table 2). Higher pH values (i.e., >7.8) were spatially measured in the headwater streams and the Hanjiang catchments (see Fig. 1a for location). In comparison, the tributaries in the southern part of the watershed exhibited relatively lower pH values. For the mainstream (Table 2), the median pH showed a significant downstream decrease from 8.29 to 7.55 ( $r^2 = 0.77$ ;  $p < 0.001$ ). The alkalinity varied from 415 to >3400  $\mu\text{mol L}^{-1}$  (Fig. 3a). Higher alkalinity (i.e., >2500  $\mu\text{mol L}^{-1}$ ) was observed in the upper reach and the upper part of the middle reach (Fig. 3a), in particular the carbonate-rich tributary catchments (e.g., the Jialingjiang, Wujiang, and Hanjiang rivers). In contrast, the lower part of the middle reach (mainly the Ganjiang River) and the lower reach showed a lower alkalinity of <2000  $\mu\text{mol L}^{-1}$ . The average alkalinity over the whole watershed was  $2210 \pm 1023 \mu\text{mol L}^{-1}$ .

#### Figure 3 and Table 2

The calculated  $p\text{CO}_2$  varied by a magnitude of 2 with the highest  $p\text{CO}_2$  being 24,432  $\mu\text{atm}$ . At 95% of the stations, the  $p\text{CO}_2$  was higher than 1000  $\mu\text{atm}$ , generally 2–20 folds the atmospheric  $p\text{CO}_2$ . Only one station in the upper reach showed a median  $p\text{CO}_2$  lower than the atmosphere. In the mainstream, the  $p\text{CO}_2$  increased from  $\sim 700 \mu\text{atm}$  at the uppermost station to 3800  $\mu\text{atm}$  at Nanjing near the river mouth (Table 2). Averaged over all stations, the basin-wide  $p\text{CO}_2$  was  $2662 \pm 1240 \mu\text{atm}$ . To better illustrate its spatial variability, we modeled the  $p\text{CO}_2$  for the whole



stream network using the Kriging interpolation method in ArcGIS 10.1 (Esri, USA) with the  
195 assumption that the station-based  $p\text{CO}_2$  was representative of the surrounding streams. Similar to  
alkalinity, the  $p\text{CO}_2$  presented significant spatial variations (Fig. 3b). The Yangtze mainstream  
near the headwater region and the Yalongjiang catchment showed the lowest  $p\text{CO}_2$ , generally  
<1000  $\mu\text{atm}$ . In comparison, the carbonate-rich tributaries in the southern part of the watershed  
had high  $p\text{CO}_2$  values. With carbonates occupying 83% of the catchment, the Wujiang River  
200 presented the highest median  $p\text{CO}_2$  than other tributaries, averaging  $3550 \pm 1356 \mu\text{atm}$ . In the  
lower reach, the  $p\text{CO}_2$  was  $3988 \pm 1244 \mu\text{atm}$  on average, which is inconsistent with its relatively  
low alkalinity of  $<2000 \mu\text{mol L}^{-1}$  (Fig. 3a). It is worth noting that the  $p\text{CO}_2$  in Hanjiang  
catchment was lower than expected, given its high alkalinity ( $>2500 \mu\text{mol L}^{-1}$ ). Differences in  
pH in these catchments are likely a principal cause of these inconsistencies.

205

In addition, the  $p\text{CO}_2$  also showed strong temporal variability. Fig. 4 presents an example of  
 $p\text{CO}_2$  changes at Datong station on the mainstream. Despite considerable inter-annual variations  
that could change by a factor of 5, the annual  $p\text{CO}_2$  declined steadily during the >20-year-long  
sampling period ( $r^2 = 0.18$ ;  $p < 0.05$ ) (Fig. 4a). This trend is pronounced even if the anomalously  
210 high values in the late 1960s are excluded from analysis. Indeed, more than half of the evaluated  
stations, mainly in the middle-lower reach, showed a significant decreasing trend at the 95%  
confidence level. In contrast, gradual increases were observed at some tributary stations in the  
upper reaches. Seasonally, the  $p\text{CO}_2$  in the wet season was on average 30% higher than that in  
the dry season (Fig. 4b), and greater fluctuation ranges could be observed in the wet season.



215

### Figure 4

#### 3.2 Correlations with hydro-geochemical variables

Fig. 5 presents two representative examples showing responses of alkalinity and  $p\text{CO}_2$  to hydrological regimes. Changes of alkalinity at both stations reflected a clear dilution effect. High alkalinity concentrations were measured in low flow periods when groundwater was the major contributor to runoff (Figs. 5a and 5c). Checking all stations indicated that the alkalinity at 98% of the stations decreased exponentially with increasing water discharge after the onset of the wet season. In contrast, the  $p\text{CO}_2$  presented diverse relationships with water changes (Figs. 5b and 5d). There was no discernible dependence of  $p\text{CO}_2$  on flow in the mainstream, while a positive correlation was widely observed in small tributaries. Although only two stations were plotted here, these diverse responses of alkalinity and  $p\text{CO}_2$  to flow changes were widespread within the watershed, in particular for  $p\text{CO}_2$  between mainstream and small tributaries.

220  
225

### Figure 5

In order to elucidate the impacts of rock weathering on  $p\text{CO}_2$ , we selected three typical tributary catchments with differing rock compositions (Table 3). The Wujiang catchment is mainly underlain by carbonates (83%) and the Ganjiang catchment by silicates (65%), whereas the Jialingjiang catchment lies in the middle regarding the areal coverage of the two rocks (Table 3 and Fig. 1b). As the most typical weathering products of carbonate and silicate rocks, we plotted  $\text{Ca}^{2+}$  and dissolved silica (expressed as  $\text{SiO}_2$ ) against  $p\text{CO}_2$ , respectively (Fig. 6). For the three catchments with contrasting rock compositions, the  $p\text{CO}_2$  showed different responses to  $\text{Ca}^{2+}$  and  $\text{SiO}_2$ . In Wujiang catchment, the log-transformed  $p\text{CO}_2$  (i.e.,  $\lg(p\text{CO}_2)$ ) presented a significant

230  
235



negative correlation with  $\text{Ca}^{2+}$  concentration ( $p < 0.001$ ) (Fig. 6). This negative correlation became less apparent with decreasing carbonate coverage in Jialingliang and Ganjiang catchments. In contrast, while the  $\lg(p\text{CO}_2)$  showed positive correlation with  $\text{SiO}_2$  in Jialingjiang and Ganjiang catchments characterized by high silicate coverage, no clear relation between  $\lg(p\text{CO}_2)$  and  $\text{SiO}_2$  was detected in Wujiang catchment (Fig. 6).

### Figure 6 and Table 3

## 4. Discussion

### 4.1 Uncertainty analysis of $p\text{CO}_2$

As an important parameter for  $\text{CO}_2$  evasion estimation, an accurate riverine  $p\text{CO}_2$  is essential to quantify  $\text{CO}_2$  evasion and explore its biogeochemical implications for carbon cycle at different scales. Compared with direct measurement by means of membrane equilibration or headspace technique, the conventional  $p\text{CO}_2$  calculation from alkalinity has been criticized for causing biases (Long et al., 2015; Hunt et al., 2011). Huge overestimations (i.e., >100%) have been reported in rivers with organic-rich and acidic waters due to combined effects of high organic acids and low buffering capacity of carbonate systems at low pH (Abril et al., 2015).

Unfortunately, there were no organic carbon information in the yearbooks, and measurements of dissolved organic carbon (DOC) in the Yangtze River started in the early 1980s. Its DOC ranging from 1.3 to 1.5  $\text{mg L}^{-1}$  was relatively low compared with other major world rivers (Bao et al., 2015; Wang et al., 2012). Our recent sampling also shows that the mean DOC is 1.9  $\text{mg L}^{-1}$  for the mainstream and 2.4  $\text{mg L}^{-1}$  for major tributaries (Liu et al., 2016). Given the neutral to basic pH range and the alkalinity variations, we believe the impact of organic acids is minimal,



although a slight overestimation may have occurred as suggested by Abril et al. (2015). Our recent  $p\text{CO}_2$  measurements in the mainstream and major tributaries using a membrane contactor (Qubit  $\text{DCO}_2$  System, Qubit Biology Inc., Canada) also indicate that the calculated  $p\text{CO}_2$  results  
260 are consistent with the measured values with only ~8% differences (Liu et al., 2016).

Furthermore, this  $p\text{CO}_2$  calculation method is sensitive to pH changes. High accuracy of pH measurements is critical to reduce the associated uncertainty. Similar to other water chemistry records (i.e., Butman and Raymond, 2011; Lauerwald et al., 2015; Weyhenmeyer et al., 2015),  
265 the retrieved pH was reported with a precision of one decimal place. If the uncertainties in pH measurement accuracy are assumed to 0.1 pH units, the calculated  $p\text{CO}_2$  would be underestimated by 26% or overestimated by 21%. To minimize human-induced disturbances in the chemical equilibrium of natural waters, we excluded the samples with  $\text{pH} < 6.5$  and treated them as being significantly polluted. Taking into account the higher alkalinity than the  
270 GEMS/Water Programme results, the propagated uncertainty ranges from 14% (underestimation) to 27% (overestimation). The Yangtze River basin is China's major industrial and agricultural regions, and influences of human activity, such as sewage inputs and chemical fertilizer usage to a lesser extent, may have altered the river water's chemical compositions and pH. As a result, 498 measurements were discarded from the analysis. Overall, for the Yangtze River with a high  
275 buffering capacity of carbonate alkalinity and low DOC concentrations, the calculated  $p\text{CO}_2$  is reasonable and can be used for further  $\text{CO}_2$  evasion estimation.



#### 4.2 Environmental impacts on alkalinity and $p\text{CO}_2$

Export of alkalinity in river systems was affected by hydrological regime with a clear dilution  
280 effect (Fig. 5). The average alkalinity was 35% lower in the wet season than in the dry season. In  
both the mainstream and the tributaries, the higher alkalinity during low flow periods in the dry  
season (Figs. 5a and 5c) illustrated the contribution of groundwater recharge in providing  
abundant alkalinity. With widespread carbonate presence, groundwater in the Yangtze River  
watershed was rich in dissolved inorganic carbon (DIC). Recent studies show that the alkalinity  
285 of typical karst groundwater in the watershed is in the range of 3300–4200  $\mu\text{mol L}^{-1}$  (Li et al.,  
2010b; Li et al., 2010a). With reduced relative contribution of groundwater in the wet season, the  
high alkalinity was diluted by local rain events that carried lower DIC contents. Spatially, the  
dilution effect was more pronounced in the upper reach than the middle-lower reach. This may  
have revealed the response of alkalinity production to land cover. Catchments with a higher  
290 forest cover normally exhibit a stronger dilution effect than cropland catchments (Raymond and  
Cole, 2003). While cropland was the major land use type in the middle-lower reach accounting  
for 53.5% of the total catchment area, forest cover in the upper Yangtze River watershed was  
much higher (37.3%) than the middle-lower reach (30.4%; data are from Data Center for  
Resources and Environmental Sciences for the 1980s).

295

Riverine dissolved  $\text{CO}_2$  originates primarily from terrestrial ecosystem respiration, groundwater  
input, and in-stream processing of land-derived organic matter (Wallin et al., 2013; Lynch et al.,  
2010). Different from alkalinity showing a clear dilution effect, the stable  $p\text{CO}_2$  in the Yangtze



mainstream likely reflected the impacts of different biogeochemical processes in maintaining its  
300  $p\text{CO}_2$  (Fig. 5b). Compared to the dry season in which the  $p\text{CO}_2$  was mainly controlled by DIC  
inputs from groundwater, the elevated  $p\text{CO}_2$  in the wet season suggested the influence of organic  
carbon transport and decomposition. Its organic carbon content in the wet season is higher and  
the age is younger due primarily to strong erosion and leaching of recent-fixed organic matter  
(Wang et al., 2012; Zhang et al., 2014). Rapid mineralization of the labile fraction of organic  
305 carbon can increase the  $p\text{CO}_2$ . For instance, approximately 60% of the recent-fixed carbon  
entering the Yangtze River can be quickly degraded in the wet season, while the degradation  
ratio in the dry season is only 31% (Wang et al., 2012). On the other hand, the increasing  $p\text{CO}_2$   
with flow in tributaries (Fig. 5d) indicated enhanced supply of fresh dissolved  $\text{CO}_2$  during high  
flow periods. For tributaries with more homogeneous catchment environments, decomposition of  
310 soil organic matter can provide abundant dissolved  $\text{CO}_2$  (Liu et al., 2016; Li et al., 2012), thus  
generating a positive  $p\text{CO}_2$  response to flow changes. From this perspective, the stable  $p\text{CO}_2$  in  
the mainstream implied that the enhanced dissolved  $\text{CO}_2$  input by soil organic matter  
decomposition from one region has likely been counteracted by low  $p\text{CO}_2$  waters derived from  
other regions. Consequently, the  $p\text{CO}_2$  dynamics appeared to be independent of hydrograph. This  
315 is highly possible given the spatial heterogeneity of the watershed environment in terms of  
vegetation cover, soil type, and rainfall intensity.

The spatial distribution of alkalinity overlapped well with the carbonate outcrops (Figs. 1b and  
3a), with ~60% of the high alkalinity concentrations measured in carbonate catchments. Using



320  $\text{Ca}^{2+}$  as a proxy of rock weathering, the strong correlation between  $\text{Ca}^{2+}$  and alkalinity suggested the dominant role of weathering in controlling alkalinity and DIC export (Fig. 7). This is consistent with the significant impact of weathering on alkalinity as observed in other rivers (Raymond and Cole, 2003; Humborg et al., 2010). Particularly, given the higher susceptibility of carbonates to weathering than silicates (Goudie and Viles, 2012), the abundant carbonate

325 presence in Wujiang catchment helped to sustain its high alkalinity and  $p\text{CO}_2$  (Table 3). The negative response of  $p\text{CO}_2$  to  $\text{Ca}^{2+}$  in Fig. 6 indicated that an elevated pH has probably occurred, offsetting the weathering-induced DIC inputs in affecting  $p\text{CO}_2$ . A slight pH increase would result in a reduced  $p\text{CO}_2$  as this calculation method is sensitive to pH fluctuations (Laruelle et al., 2013). The positive correlation between  $p\text{CO}_2$  and  $\text{SiO}_2$  in Jialingjiang and Ganjiang catchments

330 demonstrated the impact of DIC export by silicate weathering. Despite the high silicate weathering rate in Ganjiang catchment, its alkalinity represented only one third of that in the other two catchments (Table 3). Apparently, its high  $p\text{CO}_2$  of  $2642 \pm 626 \mu\text{atm}$  was primarily due to its low pH (~6% lower). Overall, the catchments with more carbonate presence presented higher  $p\text{CO}_2$  values (Figs. 1 and 3b).

335 **Figure 7**

Because  $p\text{CO}_2$  was calculated from alkalinity, its spatial variability reflected largely the export of the latter. The inconsistencies between  $p\text{CO}_2$  and alkalinity in Hanjiang catchment were likely caused by dam operation (Fig. 3). By altering the physical and biogeochemical properties of flowing water, dam trapping could cause a greatly declined  $p\text{CO}_2$  as a result of photosynthetic

340  $\text{CO}_2$  fixation and increased pH (Ran et al., 2015a). The Danjiangkou Reservoir (storage: 17.5





km<sup>3</sup>) on the upper Hanjiang River was constructed in 1968. Unfortunately, the retrieved data for the Hanjiang River started from the 1970s, rendering it impossible to compare the  $p\text{CO}_2$  differences between pre- and post-dam periods. An indirect evidence is that an elevated pH within the reservoir has been measured (7.95–8.33; Li et al., 2009) relative to the 1970s  
345 (7.84±0.15). In the lower reach near the estuary (Fig. 3b), heterotrophic ecosystems and human activity could explain its high  $p\text{CO}_2$ . Settling down of particulate organic matter coupled with nutrient-rich water plume from offshore can accelerate  $\text{CO}_2$  production. Chen et al. (2008) concluded that aerobic respiration of heterotrophic ecosystems was the primary determinant of the high  $p\text{CO}_2$  in the inner Yangtze estuary. Moreover, the lower Yangtze River basin was highly  
350 populated. Inputs of acids from agricultural fertilizer, sewage, and acid deposition have also decreased pH and shifted the carbonate system towards  $\text{CO}_2$  (Duan et al., 2007; Chen et al., 2002), generating high  $p\text{CO}_2$  values regardless of its relatively low alkalinity.

#### 4.3 Geomorphological controls on alkalinity and $p\text{CO}_2$

355 To illustrate the geomorphological controls, the used 339 stations were aggregated by stream order based on their spatial positions. Both alkalinity and  $p\text{CO}_2$  showed a decreasing trend from the smallest headwater streams through tributaries to the Yangtze mainstream (Fig. 8). The average decrease of alkalinity and  $p\text{CO}_2$  were  $94 \mu\text{mol L}^{-1}$  and  $266 \mu\text{atm}$ , respectively. Higher alkalinity and  $p\text{CO}_2$  in the headwater streams reveal the significance of direct terrestrial inputs of  
360 organic carbon and dissolved  $\text{CO}_2$  in controlling riverine carbon cycle. Over the study period, the Yangtze River watershed suffered severe soil erosion, averaging  $2167 \text{ km}^{-2} \text{ yr}^{-1}$  (Wang et al.,



2007b). Huge amounts of carbon were transported into the river system via erosion (Wu et al., 2007). Consequently, soil respiration and decomposition of the terrestrial-origin organic carbon have resulted in the CO<sub>2</sub> excess in the headwater streams (Li et al., 2012).

365

### Figure 8

The decreasing  $p\text{CO}_2$  with increasing stream order imply continued CO<sub>2</sub> evasion along the river continuum and reduced supply of fresh CO<sub>2</sub>. Except the three lakes connected to the mainstream (Fig. 1a), the Yangtze River network is largely confined to its channel. Without large floodplains supplying labile organic matter to sustain high  $p\text{CO}_2$  as in the Amazon River (Mayorga et al., 2005), its  $p\text{CO}_2$  decreased progressively from the headwaters towards the mainstream. In addition, it is interesting to note that the  $p\text{CO}_2$  in the highest three orders was equivalent (~1800  $\mu\text{atm}$ ; Fig. 8). Instead of continuous decline, the stable  $p\text{CO}_2$  suggests a balance between CO<sub>2</sub> evasion and supply of fresh CO<sub>2</sub> from upstream catchments or aquatic respiration. Contrary to the headwater streams with close contact with terrestrial ecosystems, the downstream large streams and rivers are far away from rapid fresh CO<sub>2</sub> input. Moreover, these large streams and rivers are generally characterized by low gas transfer velocity owing to weakened turbulence and mixing with benthic substrates (Butman and Raymond, 2011; Borges et al., 2015). This can effectively inhibit CO<sub>2</sub> degassing and therefore maintain the balance.

380 It is important to note, however, that the delineated 8 stream orders may not necessarily represent the actual stream network. Limited by spatial resolution, the smallest headwater streams might have been missed from the identified river network. In addition, these headwater streams are also



generally absent of sampling stations. With much closer biogeochemical interactions with land ecosystems, these missed headwater streams tend to have higher  $p\text{CO}_2$  (Benstead and Leigh, 385 2012; Aufdenkampe et al., 2011). Thus, the actual  $p\text{CO}_2$  gradient along the stream order may be sharper if a higher  $p\text{CO}_2$  in the headwater streams is included.

#### 4.4 Implications for riverine $\text{CO}_2$ evasion

As mentioned earlier, riverine carbon transport has been a significant component of carbon cycle. 390 Quantifying riverine carbon export is essential to better evaluate global carbon budget and elucidate the magnitude of carbon exchange between different carbon pools. For the estimation of  $\text{CO}_2$  evasion, riverine  $p\text{CO}_2$  denotes  $\text{CO}_2$  concentration gradient across the water-air interface and thus the potential of  $\text{CO}_2$  exchange. Prior studies indicate that elevated riverine  $p\text{CO}_2$  can enhance  $\text{CO}_2$  evasion due to a steeper concentration gradient and a greater  $\text{CO}_2$  availability for 395 degassing (Long et al., 2015; Billett and Moore, 2008). When assessing global-scale  $\text{CO}_2$  evasion, however, the spatial distribution of  $p\text{CO}_2$  is heavily skewed towards Northern America, Europe, and Australia (e.g., Lauerwald et al., 2015; Raymond et al., 2013), while data for Asian rivers are extremely lacking. This absence of an equally distributed  $p\text{CO}_2$  database has made it challenging to accurately estimate global  $\text{CO}_2$  evasion. The role of Asian rivers in global carbon export 400 explicitly demonstrates that under-representation of Asian rivers would cause huge biases.

Comparing the Yangtze River with other rivers shows that its  $p\text{CO}_2$  is higher than most world rivers (Table 4). The average  $p\text{CO}_2$  of 2662  $\mu\text{atm}$  suggests that the Yangtze River waters are



potentially a prominent carbon source for the atmosphere. Large CO<sub>2</sub> evasion fluxes have been  
405 reported by several small-scale studies in the upper reach and the estuary (Zhai et al., 2007; Chen  
et al., 2008; Li et al., 2012), as also shown in Table 4. Nonetheless, a systematic estimation of  
CO<sub>2</sub> evasion from the whole Yangtze River network, including mainstream and its tributaries of  
all orders, remains lacking. This has further hampered the assessment of its CO<sub>2</sub> evasion in a  
wider context linking the watershed's land-atmosphere and land-ocean carbon exchanges.

410 **Table 4**

Accelerated human activity is another urgent issue to be considered when investigating its  
riverine *p*CO<sub>2</sub> and CO<sub>2</sub> evasion. Approximately 50,000 dams, including the world's largest  
reservoir (i.e., the Three Gorges Reservoir; TGR), have been constructed in recent decades (Xu  
and Milliman, 2009). Assessing the impacts of dam-triggered changes to flow regime and  
415 biogeochemical processes on *p*CO<sub>2</sub> and CO<sub>2</sub> evasion is particularly important for deeper insights  
into its riverine carbon cycle (Table 4). For example, while the *p*CO<sub>2</sub> at Datong station declined  
continuously before the TGR impoundment (Fig. 4a; Wang et al., 2007a), our recent field survey  
shows that it has recovered from 1440 μatm in the 1980s to present 1700 μatm (see Fig. 4a). As  
for CO<sub>2</sub> degassing, recent work in the TGR indicates that its CO<sub>2</sub> evasion fluxes are different  
420 from natural rivers and are higher than other temperate reservoirs (Table 4; Zhao et al., 2013).  
Future research efforts are warranted to conduct systematic monitoring and evasion estimation.  
Given the Yangtze River's role in global carbon export, a comprehensive assessment of CO<sub>2</sub>  
evasion is also meaningful for global carbon budget.



## 425 Conclusions

The degassing of CO<sub>2</sub> from inland waters was recently incorporated into assessments of the global carbon budget. Because direct degassing measurements are time-consuming and unrealistic at large spatial scales, CO<sub>2</sub> efflux from aquatic systems is generally estimated from the water-air gradient of *p*CO<sub>2</sub> and gas transfer velocity. As an important parameter for

430 calculating CO<sub>2</sub> evasion, riverine *p*CO<sub>2</sub> is affected by a variety of factors and could vary substantially over space and time. Based on water chemistry data measured in the Yangtze River basin during the period 1960s–1985, we calculated the *p*CO<sub>2</sub> from pH and alkalinity. The pH in the Yangtze River waters varied from 6.5 to 9.2 and the alkalinity ranged from 415 to >3400 μmol L<sup>-1</sup> with high alkalinity concentrations occurring in carbonate-rich tributary catchments.

435 Except one station in the upper reach showing a lower *p*CO<sub>2</sub> than the atmosphere, the Yangtze River waters were supersaturated with dissolved CO<sub>2</sub>, generally 2–20 folds the atmospheric equilibrium. Averaged over all stations, the basin-wide *p*CO<sub>2</sub> was 2662±1240 μatm.

The observed spatial and temporal variations of *p*CO<sub>2</sub> were collectively controlled by terrestrial

440 ecosystems, hydrological regime, and rock weathering. High *p*CO<sub>2</sub> values were observed spatially in catchments with abundant carbonate presence and seasonally in the wet season when recent-fixed organic matter was flushed into the river network. Decomposition of organic matter by microbial activity in aquatic systems facilitated CO<sub>2</sub> production and sustained the high *p*CO<sub>2</sub> values in the wet season, although the alkalinity presented a significant dilution effect with water

445 discharge. In addition, the *p*CO<sub>2</sub> decreased with increasing stream orders from the smallest



headwater streams through tributaries to the mainstream. A higher  $p\text{CO}_2$  in the headwater streams illustrated the influence of direct inputs of terrestrially-derived organic matter and weathering products via erosion and flushing on riverine carbon dynamics.

450 The substantially higher  $p\text{CO}_2$  than the atmosphere indicated a potential of significant  $\text{CO}_2$  evasion from the Yangtze River fluvial network. Estimating the amount of  $\text{CO}_2$  evasion should be a top priority, upon which its biogeochemical implications for watershed-scale carbon cycle can be assessed in association with carbon burial and downstream export. Given the significant anthropogenic perturbations in recent decades, special attention must be paid to the resulting

455 changes to riverine  $p\text{CO}_2$  and  $\text{CO}_2$  evasion. Considering the Yangtze River's relevance to global carbon export, quantifying its  $\text{CO}_2$  evasion is of paramount importance for better assessments of global carbon budget.

460 **Acknowledgements:** This work was financially supported by the National University of Singapore (grants R-109-000-172-646 and R-109-000-191-646).

#### References

- 465 Abril, G., Bouillon, S., Darchambeau, F., Teodoru, C., Marwick, T., Tamooh, F., Omengo, F., Geeraert, N., Deirmendjian, L., Polensaere, P., and Borges, A. V.: Technical Note: Large overestimation of  $p\text{CO}_2$  calculated from pH and alkalinity in acidic, organic-rich freshwaters, *Biogeosciences*, 12, 67-78, 2015.
- Alekin, O. A., Semenov, A. D., and Skopintsev, B. A.: *Handbook of Chemical Analysis of Land Waters*, Gidrometeoizdat, St. Petersburg, Russia, 1973.
- 470 Alin, S. R., Rasera, M. d. F. F. L., Salimon, C. I., Richey, J. E., Holtgrieve, G. W., Krusche, A. V., and Snidvongs, A.: Physical controls on carbon dioxide transfer velocity and flux in low-gradient river systems and implications for regional carbon budgets, *Journal of Geophysical Research*, 116, G01009, doi: 10.1029/2010jg001398, 2011.
- American Public Health Association (APHA): *Standard Methods for the Examination of Water and Wastewater*, 16th edition, American Public Health Association, Washington, DC, 1985.



- 475 Amiotte-Suchet, P. A., Probst, J. L., and Ludwig, W.: Worldwide distribution of continental rock lithology: Implications for the atmospheric/soil CO<sub>2</sub> uptake by continental weathering and alkalinity river transport to the oceans, *Global Biogeochemical Cycles*, 17, 1038, doi: 10.1029/2002gb001891, 2003.
- 480 Aufdenkampe, A. K., Mayorga, E., Raymond, P. A., Melack, J. M., Doney, S. C., Alin, S. R., Aalto, R. E., and Yoo, K.: Riverine coupling of biogeochemical cycles between land, oceans, and atmosphere, *Front Ecol Environ*, 9, 53-60, 2011.
- Bao, H., Wu, Y., and Zhang, J.: Spatial and temporal variation of dissolved organic matter in the Changjiang: fluvial transport and flux estimation, *Journal of Geophysical Research: Biogeosciences*, 120, 1870-1886, 2015.
- 485 Barros, N., Cole, J. J., Tranvik, L. J., Prairie, Y. T., Bastviken, D., Huszar, V. L., Del Giorgio, P., and Roland, F.: Carbon emission from hydroelectric reservoirs linked to reservoir age and latitude, *Nat Geosci*, 4, 593-596, 2011.
- Battin, T. J., Luysaert, S., Kaplan, L. A., Aufdenkampe, A. K., Richter, A., and Tranvik, L. J.: The boundless carbon cycle, *Nat Geosci*, 2, 598-600, 2009.
- 490 Benstead, J. P., and Leigh, D. S.: An expanded role for river networks, *Nature Geosci*, 5, 678-679, 2012.
- Billett, M., and Moore, T.: Supersaturation and evasion of CO<sub>2</sub> and CH<sub>4</sub> in surface waters at Mer Bleue peatland, Canada, *Hydrological Processes*, 22, 2044-2054, 2008.
- 495 Borges, A. V., Darchambeau, F., Teodoru, C. R., Marwick, T. R., Tamooch, F., Geeraert, N., Omengo, F. O., Gu érin, F., Lambert, T., and Morana, C.: Globally significant greenhouse-gas emissions from African inland waters, *Nat Geosci*, 8, 637-642, 2015.
- Butman, D., and Raymond, P. A.: Significant efflux of carbon dioxide from streams and rivers in the United States, *Nat Geosci*, 4, 839-842, 2011.
- 500 Cauwet, G., and Mackenzie, F. T.: Carbon inputs and distribution in estuaries of turbid rivers: the Yang Tze and Yellow rivers (China), *Marine Chemistry*, 43, 235-246, 1993.
- Chen, C.-T. A., Zhai, W., and Dai, M.: Riverine input and air-sea CO<sub>2</sub> exchanges near the Changjiang (Yangtze River) Estuary: status quo and implication on possible future changes in metabolic status, *Continental Shelf Research*, 28, 1476-1482, 2008.
- 505 Chen, J., Wang, F. Y., Xia, X. H., and Zhang, L. T.: Major element chemistry of the Changjiang (Yangtze River), *Chemical Geology*, 187, 231-255, 2002.
- Chetelat, B., Liu, C. Q., Zhao, Z., Wang, Q., Li, S., Li, J., and Wang, B.: Geochemistry of the dissolved load of the Changjiang Basin rivers: anthropogenic impacts and chemical weathering, *Geochimica et Cosmochimica Acta*, 72, 4254-4277, 2008.
- 510 Cole, J. J., Prairie, Y. T., Caraco, N. F., McDowell, W. H., Tranvik, L. J., Striegl, R. G., Duarte, C. M., Kortelainen, P., Downing, J. A., Middelburg, J. J., and Melack, J.: Plumbing the global carbon cycle: Integrating inland waters into the terrestrial carbon budget, *Ecosystems*, 10, 171-184, 2007.
- Duan, S., Xu, F., and Wang, L.-J.: Long-term changes in nutrient concentrations of the Changjiang River and principal tributaries, *Biogeochemistry*, 85, 215-234, 2007.



- 515 Dubois, K. D., Lee, D., and Veizer, J.: Isotopic constraints on alkalinity, dissolved organic carbon, and atmospheric carbon dioxide fluxes in the Mississippi River, *Journal of Geophysical Research: Biogeosciences*, 115, 2010.
- Gan, W. B., Chen, H. M., and Hart, Y. F.: Carbon transport by the Yangtze (at Nanjing) and Huanghe (at Jinan) Rivers, People's Republic of China, in: *Transport of Carbon and Minerals in Major World Rivers, Part 2*, edited by: E.T. Degens, S. Kempe, and Soliman, H., Mitt. Geol. Paläontol. Inst. Univ. Hamburg, SCOPE/UNEP Sonderbd., 459-470, 1983.
- 520 Goudie, A. S., and Viles, H. A.: Weathering and the global carbon cycle: Geomorphological perspectives, *Earth-Science Reviews*, 113, 59-71, 2012.
- Hope, D., Billett, M., and Cresser, M.: A review of the export of carbon in river water: fluxes and processes, *Environmental Pollution*, 84, 301-324, 1994.
- 525 Humborg, C., Mörth, C., Sundbom, M., Borg, H., Blenckner, T., Giesler, R., and Ittekkot, V.: CO<sub>2</sub> supersaturation along the aquatic conduit in Swedish watersheds as constrained by terrestrial respiration, aquatic respiration and weathering, *Global Change Biology*, 16, 1966-1978, 2010.
- 530 Hunt, C., Salisbury, J., and Vandemark, D.: Contribution of non-carbonate anions to total alkalinity and overestimation of *p*CO<sub>2</sub> in New England and New Brunswick rivers, *Biogeosciences*, 8, 3069-3076, 2011.
- Ittekkot, V.: Global trends in the nature of organic matter in river suspensions, *Nature*, 332, 436-438, 1988.
- 535 Kemenes, A., Forsberg, B. R., and Melack, J. M.: CO<sub>2</sub> emissions from a tropical hydroelectric reservoir (Balbina, Brazil), *Journal of Geophysical Research*, 116, G03004, doi: 10.1029/2010JG001465, 2011.
- Laruelle, G. G., Dürr, H., Lauerwald, R., Hartmann, J., Slomp, C., Goossens, N., and Regnier, P.: Global multi-scale segmentation of continental and coastal waters from the watersheds to the continental margins, *Hydrol Earth Syst Sc*, 17, 2029-2051, 2013.
- 540 Lauerwald, R., Hartmann, J., Moosdorf, N., Kempe, S., and Raymond, P. A.: What controls the spatial patterns of the riverine carbonate system? –A case study for North America, *Chemical Geology*, 337-338, 114-127, 2013.
- Lauerwald, R., Laruelle, G. G., Hartmann, J., Ciais, P., and Regnier, P. A.: Spatial patterns in CO<sub>2</sub> evasion from the global river network, *Global Biogeochemical Cycles*, 29, 534-554, 2015.
- 545 Lewis, E., and Wallace, D. W. R.: Program developed for CO<sub>2</sub> system calculations. ORNL/CDIAC-105, Carbon dioxide Information Analysis Center, Oak Ridge National Laboratory, Oak Ridge, TN., 1998.
- Li, S.-L., Liu, C.-Q., Li, J., Lang, Y.-C., Ding, H., and Li, L.: Geochemistry of dissolved inorganic carbon and carbonate weathering in a small typical karstic catchment of Southwest China: Isotopic and chemical constraints, *Chemical Geology*, 277, 301-309, 2010a.
- 550 Li, S., Cheng, X., Xu, Z., Han, H., and Zhang, Q.: Spatial and temporal patterns of the water quality in the Danjiangkou Reservoir, China, *Hydrological sciences journal*, 54, 124-134, 2009.





- 555 Li, S., Lu, X. X., He, M., Zhou, Y., Li, L., and Ziegler, A. D.: Daily CO<sub>2</sub> partial pressure and CO<sub>2</sub> outgassing in the upper Yangtze River basin: A case study of the Longchuan River, China, *Journal of Hydrology*, 466-467, 141-150, 2012.
- Li, S., Lu, X., and Bush, R. T.: CO<sub>2</sub> partial pressure and CO<sub>2</sub> emission in the Lower Mekong River, *Journal of Hydrology*, 504, 40-56, 2013.
- 560 Li, X.-D., Liu, C.-Q., Harue, M., Li, S.-L., and Liu, X.-L.: The use of environmental isotopic (C, Sr, S) and hydrochemical tracers to characterize anthropogenic effects on karst groundwater quality: A case study of the Shuicheng Basin, SW China, *Appl Geochem*, 25, 1924-1936, 2010b.
- Liu, S., Lu, X. X., Xia, X., Zhang, S., Ran, L., Yang, X., and Liu, T.: Dynamic biogeochemical controls on river pCO<sub>2</sub> and recent changes under aggravating river impoundment: an example of the subtropical Yangtze River, *Global Biogeochemical Cycles*, 30, 880-897, 2016.
- 565 Long, H., Vihermaa, L., Waldron, S., Hoey, T., Quemin, S., and Newton, J.: Hydraulics are a first-order control on CO<sub>2</sub> efflux from fluvial systems, *Journal of Geophysical Research: Biogeosciences*, 120, 1912-1922, 2015.
- 570 Lynch, J. K., Beatty, C. M., Seidel, M. P., Jungst, L. J., and DeGrandpre, M. D.: Controls of riverine CO<sub>2</sub> over an annual cycle determined using direct, high temporal resolution pCO<sub>2</sub> measurements, *Journal of Geophysical Research*, 115, G03016, doi: 10.1029/2009jg001132, 2010.
- Mayorga, E., Aufdenkampe, A. K., Masiello, C. A., Krusche, A. V., Hedges, J. I., Quay, P. D., Richey, J. E., and Brown, T. A.: Young organic matter as a source of carbon dioxide outgassing from Amazonian rivers, *Nature*, 436, 538-541, 2005.
- 575 Milliman, J. D., Qinchun, X., and Zuosheng, Y.: Transfer of particulate organic carbon and nitrogen from the Yangtze River to the ocean, *American Journal of Science*, 284, 824-834, 1984.
- 580 Ran, L., Lu, X. X., Richey, J. E., Sun, H., Han, J., Liao, S., and Yi, Q.: Long-term spatial and temporal variation of CO<sub>2</sub> partial pressure in the Yellow River, China, *Biogeosciences*, 12, 921-932, 2015a.
- Ran, L., Lu, X. X., Yang, H., Li, L., Yu, R., Sun, H., and Han, J.: CO<sub>2</sub> outgassing from the Yellow River network and its implications for riverine carbon cycle, *Journal of Geophysical Research: Biogeosciences*, 120, 1334-1347, 2015b.
- 585 Raymond, P. A., Caraco, N. F., and Cole, J. J.: Carbon dioxide concentration and atmospheric flux in the Hudson River, *Estuaries*, 20, 381-390, 1997.
- Raymond, P. A., Bauer, J. E., and Cole, J. J.: Atmospheric CO<sub>2</sub> evasion, dissolved inorganic carbon production, and net heterotrophy in the York River estuary, *Limnology and Oceanography*, 45, 1707-1717, 2000.
- 590 Raymond, P. A., and Cole, J. J.: Increase in the export of alkalinity from North America's largest river, *Science*, 301, 88-91, 2003.
- Raymond, P. A., Hartmann, J., Lauerwald, R., Sobek, S., McDonald, C., Hoover, M., Butman, D., Striegl, R., Mayorga, E., and Humborg, C.: Global carbon dioxide emissions from inland waters, *Nature*, 503, 355-359, 2013.



- 595 Regnier, P., Friedlingstein, P., Ciais, P., Mackenzie, F. T., Gruber, N., Janssens, I. A., Laruelle, G. G., Lauerwald, R., Luysaert, S., and Andersson, A. J.: Anthropogenic perturbation of the carbon fluxes from land to ocean, *Nat Geosci*, 6, 597-607, 2013.
- Richey, J. E., Melack, J. M., Aufdenkampe, A. K. et al.: Outgassing from Amazonian rivers and wetlands as a large tropical source of atmospheric CO<sub>2</sub>, *Nature*, 416, 617-620, 2002.
- 600 Sarma, V. V. S. S., Kumar, N. A., Prasad, V. R. et al.: High CO<sub>2</sub> emissions from the tropical Godavari estuary (India) associated with monsoon river discharges, *Geophys Res Lett*, 38, L08601, doi: 10.1029/2011gl046928, 2011.
- Schlünz, B., and Schneider, R. R.: Transport of terrestrial organic carbon to the oceans by rivers: re-estimating flux- and burial rates, *Int J Earth Sci*, 88, 599-606, 2000.
- 605 Syvitski, J. P. M., Vorosmarty, C. J., Kettner, A. J., and Green, P.: Impact of humans on the flux of terrestrial sediment to the global coastal ocean, *Science*, 308, 376-380, 2005.
- Telmer, K., and Veizer, J.: Carbon fluxes, pCO<sub>2</sub> and substrate weathering in a large northern river basin, Canada: carbon isotope perspectives, *Chemical Geology*, 159, 61-86, 1999.
- Teodoru, C., Nyoni, F., Borges, A., Darchambeau, F., Nyambe, I., and Bouillon, S.: Dynamics of greenhouse gases (CO<sub>2</sub>, CH<sub>4</sub>, N<sub>2</sub>O) along the Zambezi River and major tributaries, and their importance in the riverine carbon budget, *Biogeosciences*, 12, 2431-2453, 2015.
- 610 Wallin, M. B., Grabs, T., Buffam, I., Laudon, H., Ågren, A., Öquist, M. G., and Bishop, K.: Evasion of CO<sub>2</sub> from streams—The dominant component of the carbon export through the aquatic conduit in a boreal landscape, *Global Change Biology*, 19, 785-797, 2013.
- 615 Wang, F. S., Wang, Y. C., Zhang, J., Xu, H., and Wei, X. G.: Human impact on the historical change of CO<sub>2</sub> degassing flux in River Changjiang, *Geochem T*, 8, 2007a.
- Wang, F. S., Wang, B. L., Liu, C. Q., Wang, Y. C., Guan, J., Liu, X. L., and Yu, Y. X.: Carbon dioxide emission from surface water in cascade reservoirs-river system on the Maotiao River, southwest of China, *Atmos Environ*, 45, 3827-3834, 2011.
- 620 Wang, X., Ma, H., Li, R., Song, Z., and Wu, J.: Seasonal fluxes and source variation of organic carbon transported by two major Chinese Rivers: The Yellow River and Changjiang (Yangtze) River, *Global Biogeochemical Cycles*, 26, GB2025, doi: 10.1029/2011gb004130, 2012.
- Wang, Z. Y., Li, Y., and He, Y.: Sediment budget of the Yangtze River, *Water Resour Res*, 43, W04401, doi: 10.1029/2006WR005012, 2007b.
- 625 Wanninkhof, R., Park, G.-H., Takahashi, T., Sweeney, C., Feely, R. A., Nojiri, Y., Gruber, N., Doney, S. C., McKinley, G. A., and Lenton, A.: Global ocean carbon uptake: magnitude, variability and trends, *Biogeosciences*, 10, 1983-2000, 2013.
- Weyhenmeyer, G. A., Kosten, S., Wallin, M. B., Tranvik, L. J., Jeppesen, E., and Roland, F.: Significant fraction of CO<sub>2</sub> emissions from boreal lakes derived from hydrologic inorganic carbon inputs, *Nat Geosci*, 8, 933-936, 2015.
- 630 Wu, Y., Zhang, J., Liu, S. M., Zhang, Z. F., Yao, Q. Z., Hong, G. H., and Cooper, L.: Sources and distribution of carbon within the Yangtze River system, *Estuarine, Coastal and Shelf Science*, 71, 13-25, 2007.
- Xu, K., and Milliman, J. D.: Seasonal variations of sediment discharge from the Yangtze River before and after impoundment of the Three Gorges Dam, *Geomorphology*, 104, 276-283, 2009.
- 635



- Yang, S., Zhao, Q., and Belkin, I. M.: Temporal variation in the sediment load of the Yangtze river and the influences of human activities, *Journal of Hydrology*, 263, 56-71, 2002.
- 640 Yao, G. R., Gao, Q. Z., Wang, Z. G., Huang, X. K., He, T., Zhang, Y. L., Jiao, S. L., and Ding, J.: Dynamics of CO<sub>2</sub> partial pressure and CO<sub>2</sub> outgassing in the lower reaches of the Xijiang River, a subtropical monsoon river in China, *Sci Total Environ*, 376, 255-266, 2007.
- Zhai, W. D., Dai, M. H., and Guo, X. G.: Carbonate system and CO<sub>2</sub> degassing fluxes in the inner estuary of Changjiang (Yangtze) River, China, *Marine Chemistry*, 107, 342-356, 2007.
- 645 Zhang, L., Xue, M., Wang, M. et al.: The spatiotemporal distribution of dissolved inorganic and organic carbon in the main stem of the Changjiang (Yangtze) River and the effect of the Three Gorges Reservoir, *Journal of Geophysical Research: Biogeosciences*, 119, 741-757, 2014.
- Zhao, Y., Wu, B., and Zeng, Y.: Spatial and temporal patterns of greenhouse gas emissions from Three Gorges Reservoir of China, *Biogeosciences*, 10, 1219-1230, 2013.
- Zhu, T. X.: Gully and tunnel erosion in the hilly Loess Plateau region, China, *Geomorphology*, 153-154, 144-155, 2012.



650 Table 1. Comparison of alkalinity ( $\text{meq L}^{-1}$ ) and pH at Wuhan station between the GEMS/Water Programme results and the hydrological yearbooks, expressed as mean $\pm$ standard error.

Item	1980	1981	1982	1983	1984	1984
GEMS/Water Programme						
Alkalinity	2.05 $\pm$ 0.29	2.00 $\pm$ 0.19	2.01 $\pm$ 0.23	1.84 $\pm$ 0.25	2.20 $\pm$ 0.25	1.99 $\pm$ 0.22
pH	7.83 $\pm$ 0.16	7.73 $\pm$ 0.24	8.04 $\pm$ 0.09	8.06 $\pm$ 0.05	8.00 $\pm$ 0.09	7.88 $\pm$ 0.06
Hydrological yearbooks						
Alkalinity	2.31 $\pm$ 0.31	2.19 $\pm$ 0.24	2.27 $\pm$ 0.27	2.03 $\pm$ 0.30	2.38 $\pm$ 0.28	2.31 $\pm$ 0.24
pH	7.93 $\pm$ 0.09	7.87 $\pm$ 0.09	8.01 $\pm$ 0.09	7.94 $\pm$ 0.08	7.93 $\pm$ 0.10	7.98 $\pm$ 0.08


 Table 2. Riverine pH, alkalinity, and  $p\text{CO}_2$  in the Yangtze River basin (median±standard deviation).

River/tributary	Station	pH	Alkalinity	$p\text{CO}_2$
			$\mu\text{mol L}^{-1}$	$\mu\text{atm}$
Mainstream	Benzilan	8.29±0.11	2352±435	681±156
	Shigu	8.18±0.48	2544±438	846±262
	Jingjiangjie	8.11±0.12	2905±362	916±202
	Dukou	8.22±0.12	2399±429	826±197
	Longjie	8.23±0.17	2185±396	786±226
	Huatan	8.17±0.15	2237±418	882±287
	Pingshan	8.13±0.10	2215±407	1001±235
	Zhutuo	7.88±0.19	2299±349	2405±781
	Cuntan	8.08±0.11	2173±311	1087±319
	Yichang	7.95±0.15	2343±300	1653±469
	Luoshan	7.76±0.11	2280±248	2380±691
	Wuhan	7.93±0.11	2060±263	1521±497
	Datong	7.84±0.14	1919±312	1711±806
	Nanjing <sup>a</sup>	7.56±0.16	2339±339	3796±1623
	Nanjing <sup>b</sup>	7.54±0.18	2296±357	3793±2186
Major tributaries <sup>c</sup>				
Yalongjiang	Xiaodeshi	8.02±0.22	2576±465	1567±715
Daduhe	Fuluzhen	7.66±0.23	1909±289	2577±1620
Minjiang	Gaochang	8.02±0.15	1816±327	1020±525
Tuojiang	Lijiawan	8.01±0.11	2705±507	1504±572
Jialingjiang	Beibei	8.11±0.14	2289±509	1196±244
Wujiang	Wulong	8.01±0.14	2420±279	1361±508
Yuanjiang	Taoyuan	7.61±0.25	1822±480	2801±2144
Xiangjiang	Xiangtan	7.76±0.44	1739±331	2349±2521
Hanjiang	Xiaoshicun	7.93±0.13	2262±480	1715±536
Ganjiang	Waizhou	7.44±0.44	880±236	2205±2048
Yangtze basin <sup>d</sup>	1% percentile	7.03	556	788
	10% percentile	7.35	842	1236
	50% percentile	7.71	2237	2455
	90% percentile	8.05	3305	4344
	99% percentile	8.28	4437	6163

655

<sup>a</sup>affected by high tides.<sup>b</sup>affected by low tides.<sup>c</sup>Median values of the data for the lowermost station on the mainstream of the specific tributary.



660

<sup>d</sup>Statistics based on the measurements at the used 339 stations.

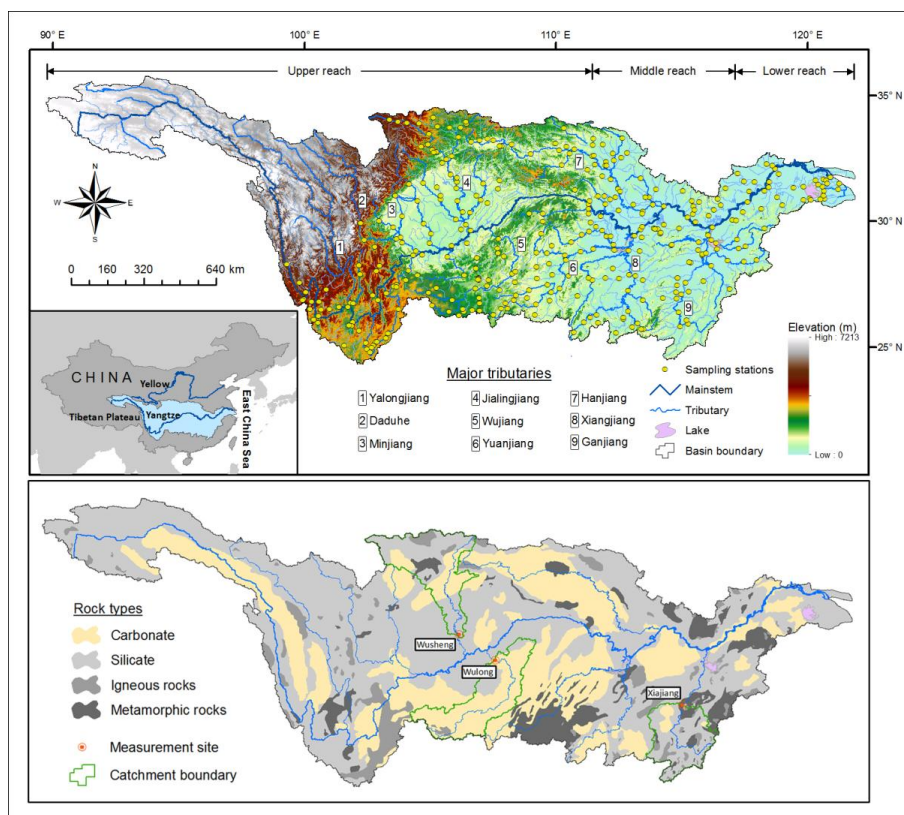
Table 3. Hydro-geochemical features of the Wujiang (Wulong station), Jialingjiang (Wusheng station), and Ganjiang (Xiajiang station) catchments.

Control station	Control area km <sup>2</sup>	Water discharge m <sup>3</sup> s <sup>-1</sup>	pH	Alkalinity	<i>p</i> CO <sub>2</sub>	Ca <sup>2+</sup>	SiO <sub>2</sub>	Rock types (% of area)		
				μmol L <sup>-1</sup>	μatm	μmol L <sup>-1</sup>	μmol L <sup>-1</sup>	Carbonate	Silicate	Igneous + metamorphic
Wulong	80,536	1570	7.72±0.14	3021±527	3537±1247	1145±278	59±31	82.9	14.8	2.3
Wusheng	80,550	793	7.80±0.21	2484±948	2671±490	1005±170	94±30	30.4	55.3	14.3
Xiajiang	62,387	1644	7.34±0.08	953±266	2642±626	242±91	105±18	9.1	64.7	26.2

665

Table 4. Comparison of *p*CO<sub>2</sub> and CO<sub>2</sub> evasion among world large rivers and typical reservoirs in the Yangtze River basin.

River	Country	Climate	<i>p</i> CO <sub>2</sub>	CO <sub>2</sub> evasion	Reference
			μatm	mol m <sup>-2</sup> yr <sup>-1</sup>	
Yangtze network	China	Subtropical monsoon	2662±1240	/	This study
Upper Yangtze	China	Subtropical monsoon	2100	57	Li et al., 2012
Lower Yangtze	China	Subtropical monsoon	1297±901	14.2–54.4	Wang et al., 2007a
Yangtze estuary	China	Subtropical monsoon	650–1440	15.5–34.2	Zhai et al., 2007
Amazon	Brazil	Tropical	3929	162.2	Lauerwald et al. 2015
Ottawa	Canada	Temperate	1200	14.2	Telmer and Veizer, 1999
Hudson	USA	Temperate	1125±403	5.8–13.5	Raymond et al., 1997
York estuary	USA	Temperate	1070±867	6.3	Raymond et al., 2000
Mississippi	USA	Temperate	1335±130	98.5±32.5	Dubois et al., 2010
Yukon	Canada	Subarctic	582–705	11.6–21.2	Lauerwald et al., 2015
Yellow	China	Arid and semiarid	2810±1985	312.4±149.2	Ran et al., 2015b
Xijiang (Pearl)	China	Subtropical monsoon	2600	69.2–130	Yao et al., 2007
Mekong (>100 m wide rivers)	SE Asia	Tropical monsoon	703–1597	32–138	Alin et al., 2011
Godavari estuary	India	Tropical monsoon	<500–33,000	52.6	Sarma et al., 2011
Global rivers			2400	131.2	Lauerwald et al. 2015
<i>Typical reservoirs in the Yangtze River basin</i>					
Wujiang cascade reservoirs			38–3300	-3.3–32.5	Wang et al., 2011
Three Gorges Reservoir (TGR)			/	35.1	Zhao et al., 2013



670 Fig. 1. Maps of the Yangtze River basin showing sampling stations (top) and rock compositions (bottom). Rock information is modified from Chen et al. (2002) and Chetelat et al. (2008).

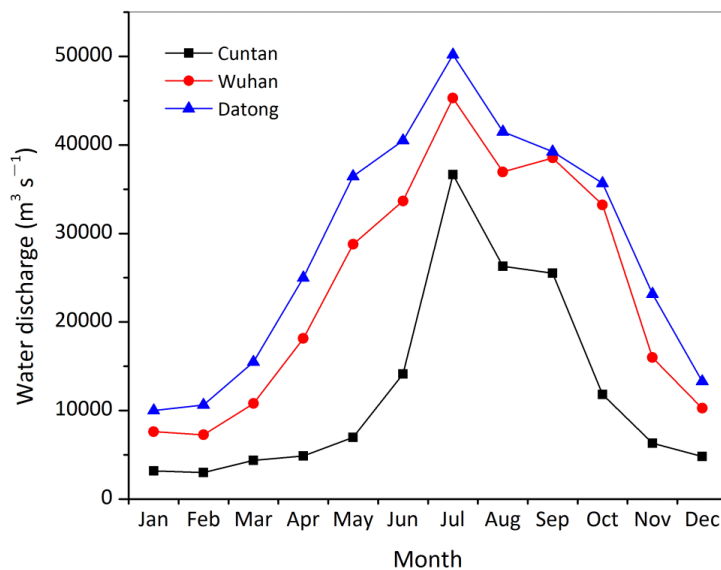


Fig. 2. Monthly variations in water discharge of the Yangtze River at Cuntan (upper reach), Wuhan (middle reach), and Datong stations (lower reach).



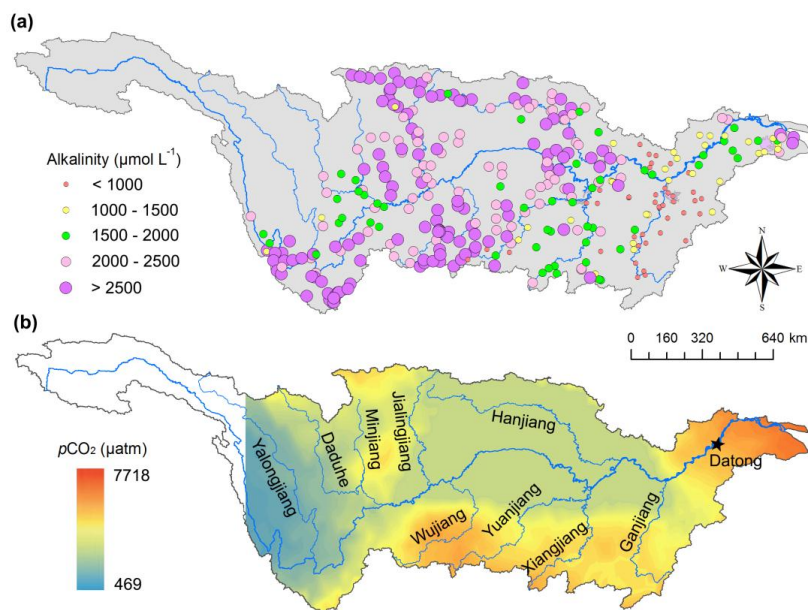
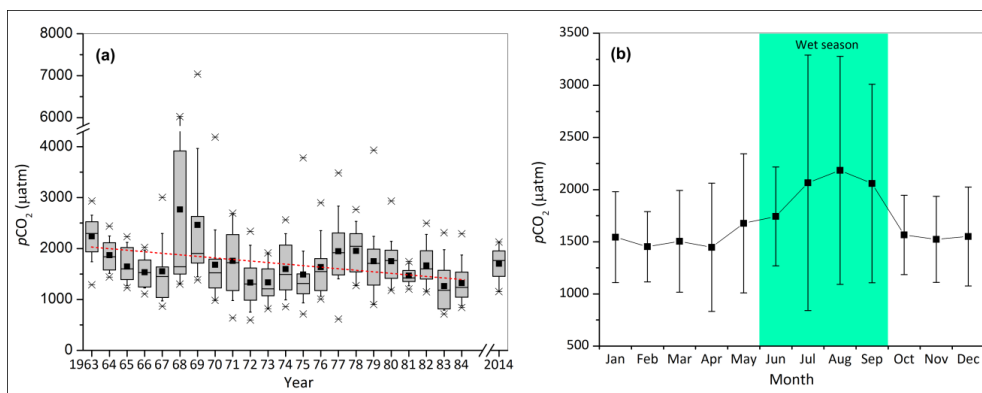
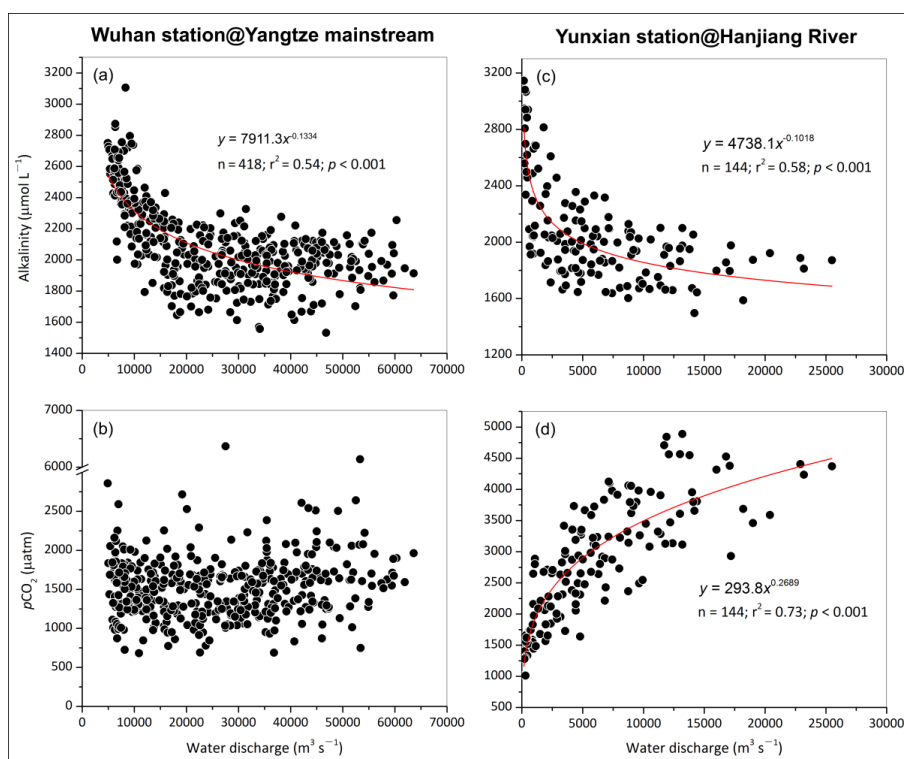


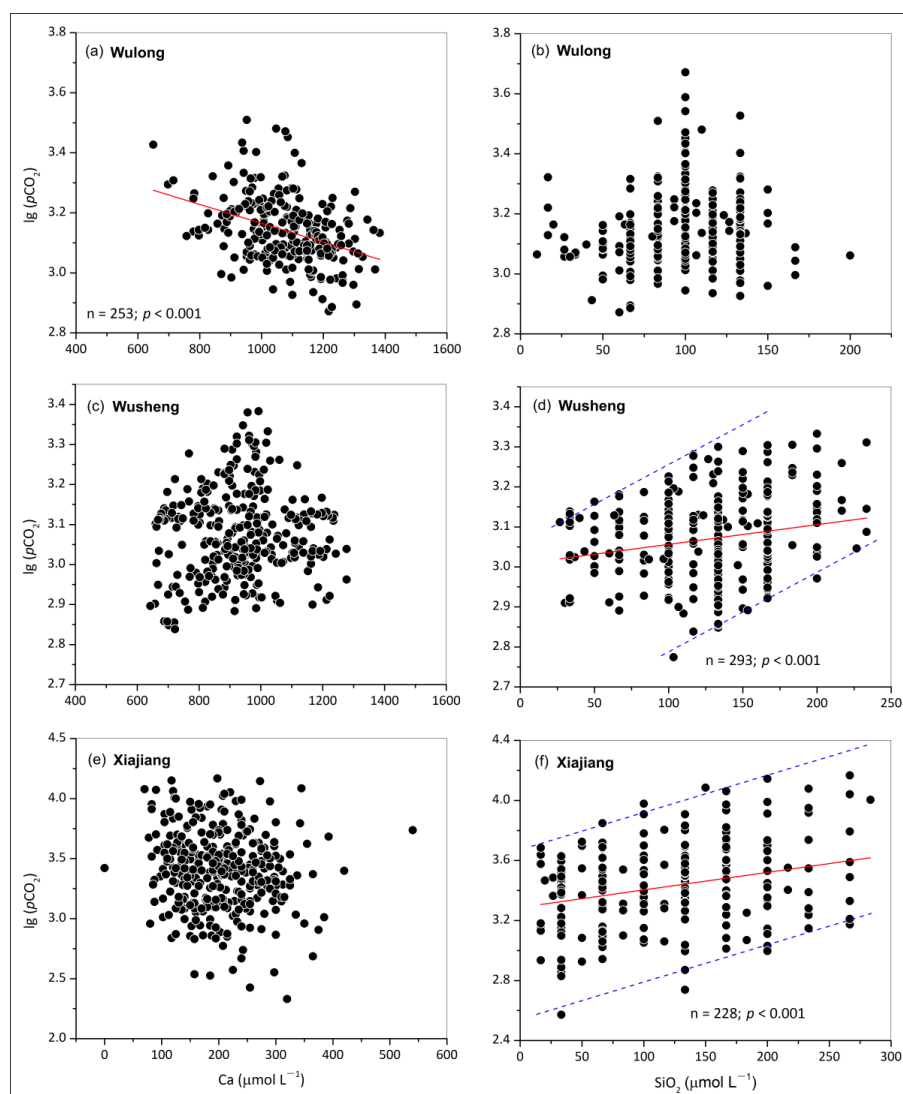
Fig. 3. Spatial distribution of alkalinity (a) and  $p\text{CO}_2$  (b) in the Yangtze River basin. The headwater region in (b) was not interpolated due to insufficient stations.



680 Fig. 4. Temporal variations of  $p\text{CO}_2$  at Datong station. (a) box-and-whisker plot shows significant inter-annual changes; (b) seasonal variations. The dash line in (a) represents linear regression and the values for 2014 are derived from Liu et al. (2016). Error bars denote standard deviation.



685 Fig. 5. Correlations between water discharge and instantaneous alkalinity and  $p\text{CO}_2$ : the  
mainstream at Wuhan station (a and b) and the Hanjiang River at Yunxian station (c and d).



690 Fig. 6. Responses of  $p\text{CO}_2$  to rock weathering products in three typical catchments with distinct rock compositions: a–b: Wujiang River (Wulong station); b–c: Jialiangjiang River (Wusheng station); e–f: Ganjiang River (Xiajiang station). The solid lines represent linear regression.

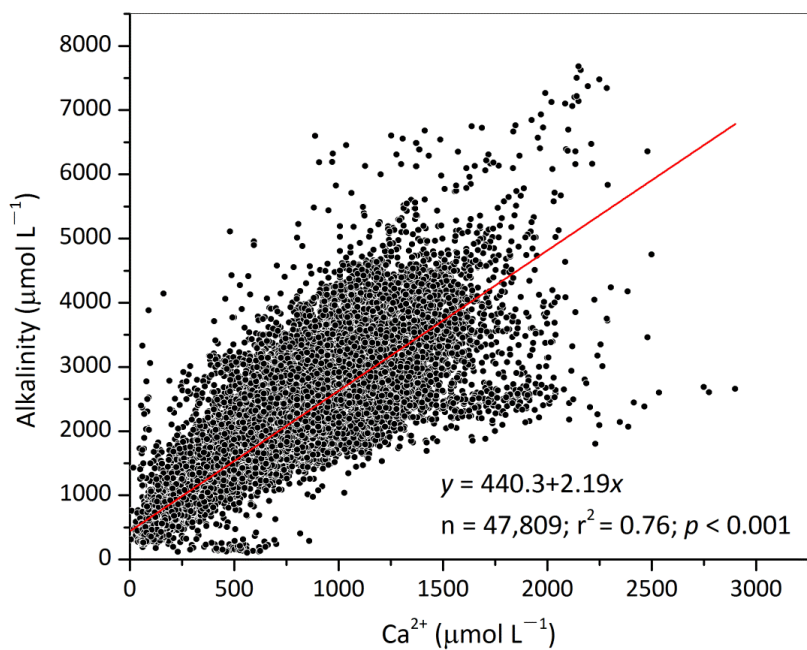


Fig. 7. Strong correlation between chemical weathering, using  $\text{Ca}^{2+}$  as a proxy, and alkalinity.

695

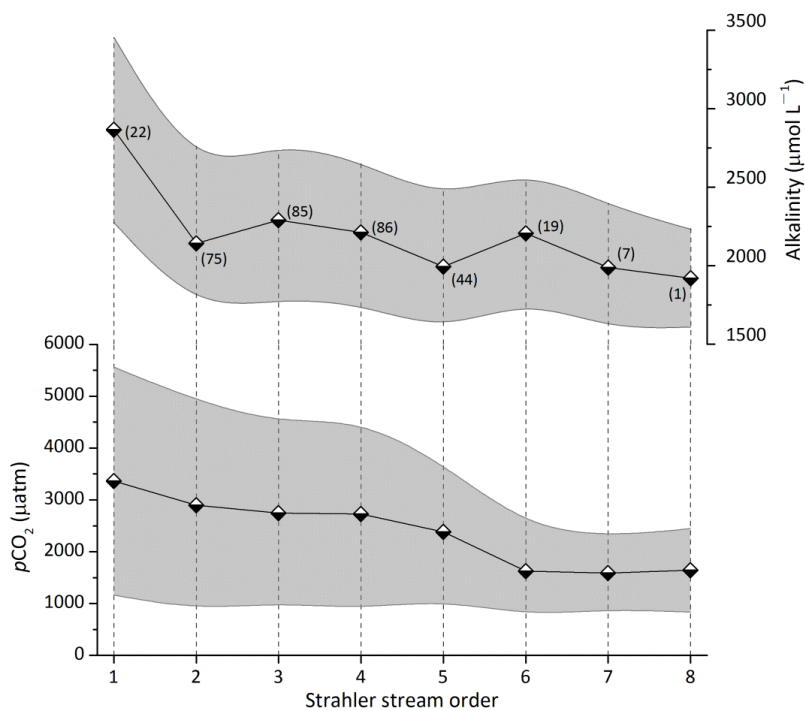


Fig. 8. Decreasing alkalinity (top) and  $p\text{CO}_2$  (bottom) with increasing Strahler stream order. The grey shade denotes standard deviation and the numbers in parentheses represent the number of stations aggregated for each stream order.